This article was downloaded by:
On: *29 January 2011*
Access details: *Access Details: Free Access*
Publisher *Taylor & Francis*
Informa Ltd Registered in England and Wales Registered Number: 1072954 Registered office: Mortimer House, 37-41 Mortimer Street, London W1T 3JH, UK

Supramolecular Chemistry
Publication details, including instructions for authors and subscription information:
http://www.informaworld.com/smpp/title~content=t713649759

Synthesis, Characterization and EPR Studies of Supramolecular Porphyrazines

Ramazan Öztürk[a]; Sadik Güner[b]; Bekir Aktaş[c]; Ahmet Gül[d]
[a] Department of Chemistry, Fatih University, Buyukcekmece, Istanbul, Turkey [b] Department of Physics, Fatih University, Buyukcekmece, Istanbul, Turkey [c] Department of Physics, Gebze Institute of Technology, Gebze, Kocaeli, Turkey [d] Department of Chemistry, Technical University of Istanbul, Maslak, Turkey

To cite this Article Öztürk, Ramazan , Güner, Sadik , Aktaş, Bekir and Gül, Ahmet(2005) 'Synthesis, Characterization and EPR Studies of Supramolecular Porphyrazines', Supramolecular Chemistry, 17: 3, 233 — 241
To link to this Article: DOI: 10.1080/10610270412331337295
URL: http://dx.doi.org/10.1080/10610270412331337295

PLEASE SCROLL DOWN FOR ARTICLE

Full terms and conditions of use: http://www.informaworld.com/terms-and-conditions-of-access.pdf

This article may be used for research, teaching and private study purposes. Any substantial or systematic reproduction, re-distribution, re-selling, loan or sub-licensing, systematic supply or distribution in any form to anyone is expressly forbidden.

The publisher does not give any warranty express or implied or make any representation that the contents will be complete or accurate or up to date. The accuracy of any instructions, formulae and drug doses should be independently verified with primary sources. The publisher shall not be liable for any loss, actions, claims, proceedings, demand or costs or damages whatsoever or howsoever caused arising directly or indirectly in connection with or arising out of the use of this material.

Supramolecular Chemistry, April–May 2005 Vol. 17 (3), pp. 233–241

Taylor & Francis
Taylor & Francis Group

Synthesis, Characterization and EPR Studies of Supramolecular Porphyrazines

RAMAZAN ÖZTÜRK[a,b], SADIK GÜNER[c], BEKIR AKTAŞ[d] and AHMET GÜL[a,*]

[a]*Department of Chemistry, Technical University of Istanbul, 34469 Maslak, Turkey;* [b]*Department of Chemistry, Fatih University, 34500 Buyukcekmece, Istanbul, Turkey;* [c]*Department of Physics, Fatih University, 34500 Buyukcekmece, Istanbul, Turkey;* [d]*Department of Physics, Gebze Institute of Technology, 41400 Gebze, Kocaeli, Turkey*

Received (in Southampton, UK) 4 June 2004; Accepted 10 November 2004

Supramolecular porphyrazines with eight pyridine donor groups bound through ethylthio ester bridges on the periphery have been prepared. The pyridine donors were quaternized with iodomethane to octacationic porphyrazine. The nonanuclear supramolecular porphyrazine was prepared by the coordination of peripheral pyridine donors with $VO(acac)_2$. The paramagnetic nonanuclear structure was studied in powder and in solution form by EPR. EPR studies together with the other spectral data confirmed the presence of identical pyridine-coordinated $VO(acac)_2$ paramagnetic centers attached to the peripheral positions of the porphyrazine core.

Keywords: Porphyrazine; Supramolecule; EPR; Vanadyl; Complex

Downloaded At: 15:13 29 January 2011

INTRODUCTION

The impressive amount of research into cationic and supramolecular macrocycles is a consequence of their possible diverse applications in nontraditional fields of technology, ranging from biology to material science and molecular electronics [1]. In biological systems, cationic porphyrins can act as singlet oxygen generators in photodynamic therapy, inhibitors of human telomerases, receptors for peptides, DNA cleavers and specific probes of DNA structures [1–11]. As cationic porphyrins have planar structures with quaternized functional groups on the peripheral positions, their activity is different from conventional intercalators such as ethidium bromide, proflavin and daunomycin [8–9]. Crystallographic analysis of a metalloporphyrin–oligonuclotide complex has shown that intercalation or binding of cationic porphyrin causes a distortion of the DNA molecule [1–7].

Cationic porphyrazines (i.e. tetraazaporphyrins) can be proposed as alternatives in the above-mentioned fields of application as they have similar properties to porphyrins and phthalocyanines and their synthesis and isolation are relatively simple. Functional groups on the peripheral positions of porphyrazines are integrated into the macrocyclic core more effectively than those of phthalocyanines [12]. Furthermore, the synthetic route to octakis-functionalized porphyrazine can be performed easily by cyclization of the functionalized maleonitrile derivatives in the presence of magnesium alkoxide (usually propanol and butanol are used). Hence, the preparation of the porphyrazine core is much easier than that of porphyrin, which is generally synthesized by the cyclization of pyrroles [13].

Supramolecular systems of porphyrinic macrocycles have also been investigated for various purposes such as molecular devices, photonic wires and construction of light-harvesting systems [14–20]. To obtain these supramolecular systems with well-defined geometries and size, porphyrinic molecules have proved to be versatile building blocks [21–25]. In the preparation of supramolecular systems the central porphyrin core with N-donors at the peripheral positions is very useful for the subsequent step of coordination to form different transition metal complexes. Substitution of pyridine groups at the peripheral positions of the porphyrin core results in noncovalent self-assembling properties useful for construction of supramolecular systems [26–30].

*Corresponding author. Tel.: +90- 212-285-6827. Fax: +90-212-285-6386. E-mail: ahmetg@itu.edu.tr

ISSN 1061-0278 print/ISSN 1029-0478 online © 2005 Taylor & Francis Group Ltd
DOI: 10.1080/10610270412331337295

Downloaded At: 15:13 29 January 2011

Inclusion of the paramagnetic units on supramolecular systems is expected to exhibit interesting properties in the field of paramagnetic materials [31]. Paramagnetic properties can be analyzed by electron paramagnetic resonance (EPR), which provides information about the elemental composition and electronic structure of paramagnetic states and nuclearity. The apparent g (Lande splitting factor) value is used to assess the spin state of the molecule. The number of hyperfine lines and the magnitude of the hyperfine coupling constant can be used to identify the nuclei to which the unpaired electrons are coupled.

The first example of a multifunctional molecule combining porphyrazine core with pyridine donors on the periphery was reported by Anderson *et al.* [13]. However, direct attachment of the pyridyl group to the porphyrazine core in their work resulted in a product with a relatively rigid structure and low solubility in common organic solvents. To overcome these difficulties, a different strategy can be proposed; as shown by Eichorn *et al.* [32] reactive functional sites on porphyrazines can be built up to further functionalize with the desired substituents. For example, hydroxyalkyl substituents could be converted to unsaturated ester units. Our group also reported porphyrazines connected to ferrocenes or benzocrown ethers through flexible ethoxyester bridges [33, 34]. A similar procedure can be applied to obtain porphyrazines with pyridyl groups attached through flexible chains, making full use of the donor properties of the pyridine moieties.

In this paper, we report the synthesis of an octacationic porphyrazine by quaternization of the pyridyl donors and a supramolecular nonanuclear porphyrazine by the coordination of those donor sites with coordinatively unsaturated $VO(acac)_2$ [35]. EPR data of the latter have been evaluated in detail.

RESULTS AND DISCUSSION

General Characterization

The synthesis route to supramolecular and octacationic porphyrazines followed a multistep sequence. The starting point was the preparation of a porphyrazine core with reactive hydroxyethylthio substituents. Thus, octakis(2-hydroxyethylthio)porphyrazinatomagnesium, MgOHPz, was synthesized as reported previously. First, 1,2-bis(2-hydroxylethylthio)maleonitrile was prepared and its cyclotetramerization in the presence of magnesium butanolate gave the dark blue product MgOHPz. The spectral data for this compound closely followed the reported data [33, 34].

The second step to the supramolecular structure was the addition of pyridyl donors on the peripheral positions of the porphyrazine unit. For this purpose, MgOHPz was reacted with pyridine-4-carboxylic acid to form ester bridges. Several ester-forming reactions were tried, but full esterification of all eight OH groups in MgOHPz with pyridine-4-carboxylic acid (isonicotinic acid) to give octakis(4-pyridoxyethylthio)porphyrazinato magnesium (MgPyPz) was accomplished in pyridine in the presence of dicyclohexylcarbodiimide (DCCI) and 4-toluenesulfonic acid (*p*-TSA) as catalysts for 7 days at ambient temperature. Here the function of DCCI was to facilitate formation of the ester bond by forming an activated ester [32]. The byproduct dicyclohexylurea was separated from the crude product by treatment with a solvent mixture of 1:1 cyclohexane/ethanol for 1 day at 0 °C and then washing with the same mixture several times. The dark green product was isolated in an adequate yield of 35% after chromatography (Fig. 1). In the FTIR spectra, the presence of C═O peaks around 1727 cm^{-1}, aromatic and aliphatic C—H peaks around 2900–3050 cm^{-1} and the disappearance of the O—H peaks around 3430 cm^{-1}, together with the high solubility in chloroform acquired after this reaction, are all evidence for the formation of MgPyPz.

In the electronic absorption spectrum of porphyrazine, Q- and B-band absorptions are the result of π—π* transitions of the pyrrole units, which are located in the central core of the porphyrazine. For the metalloporphyrazines with D_{4h} symmetry there is only a single Q-band absorption. Pyridine groups cannot affect the Q-band absorption when they are far from the central core. Consequently, there was no net difference between the electronic spectra of MgPyPz and MgOHPz. The absorption maxima of both MgOHPz and MgPyPz are around 372 and 674 nm.

In the synthesis of the metal-free porphyrazines, the general route is the treatment of magnesium porphyrazine with strong acids such as concentrated

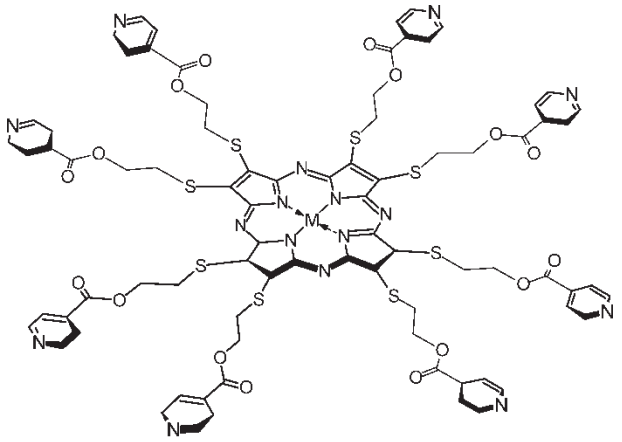

FIGURE 1 Structure of MgPyPz.

Downloaded At: 15:13 29 January 2011

sulfuric, hydrochloric or trifluoroacetic acid. In our study, demetalization of MgPyPz to the metal-free form (H_2PyPz) was accomplished by treatment of MgPyPz with 6 M H_2SO_4. The reaction was carried out at 0°C to prevent hydrolysis of the ester groups. When the dark blue MgPyPz was dissolved in a minimum amount (5 ml) of 6 M sulfuric acid, the color of the mixture turned to purple. In addition to this change in color, conversion to metal-free derivative H_2PyPz was verified for inner-core NH protons by the FTIR spectrum with a stretching absorption at 3293 cm^{-1} and also by the ^{1}H NMR spectrum with a broad chemical shift at −1.97 ppm indicating the strong shielding of the 18-π electron system.

In the electronic spectra of metal-free porphyrazine, there is a significant change in the Q-band absorption of the porphyrazine molecule due to the change in the symmetry of the molecule from D_{4h} to D_{2h}. In the electronic spectrum of the metalloporphyrazines with D_{4h} symmetry, an intense Q-band absorption in the lower energy side of the visible range is assigned to the π—π* transition of the porphyrazine core; however, this absorption is split, with one absorption at the shorter and the other at the longer wavelength, as a consequence of the decrease in symmetry to D_{2h}. In this study, the electronic absorption spectrum of H_2PyPz has two Q-band absorption maxima at 640 and 704 nm, confirming the proposed structure (Fig. 2).

For the preparation of the water-soluble octacationic molecule (QMgPyPz) (Fig. 3), the pyridine groups on the peripheral positions of MgPyPz were quaternized with iodomethane with a high yield (70%) [36].

The electronic absorption spectrum of QMgPyPz in water shows extensive similarity to the spectrum

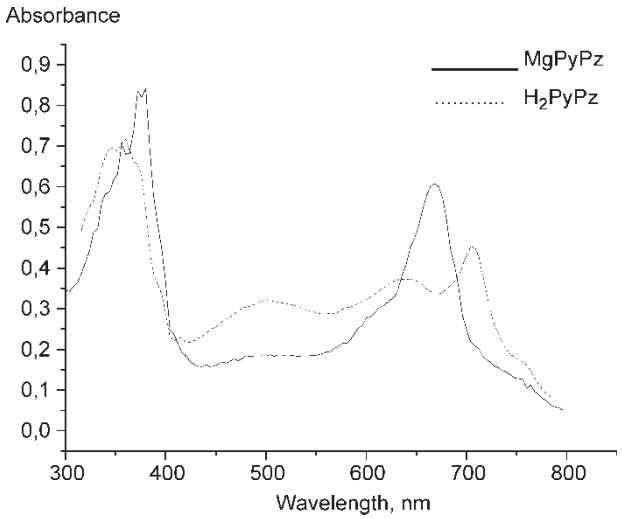

FIGURE 2 UV–vis spectra of (a) H_2PyPz and (b) MgPyPz.

of MgPyPz in chloroform although the polarities of these solvents are completely different. A qualitative test carried out by stirring a mixture of aqueous QMgPyPz solution and bovine albumin serum also indicated the interaction of the octacationic compound with proteins by a decrease in the concentration of the porphyrazine derivative in solution and the formation of a colored precipitate [9].

The primary goal of this study was the construction of a supramolecular structure starting with a porphyrazine molecule. Taking into account the ready coordination of $VO(acac)_2$ with pyridine donors [37], these penta-coordinated complexes were preferred as the capping agents for eight pyridine end-groups on each molecule to reach the nonanuclear supramolecular structure. The dark green, solid, nonanuclear supramolecular product

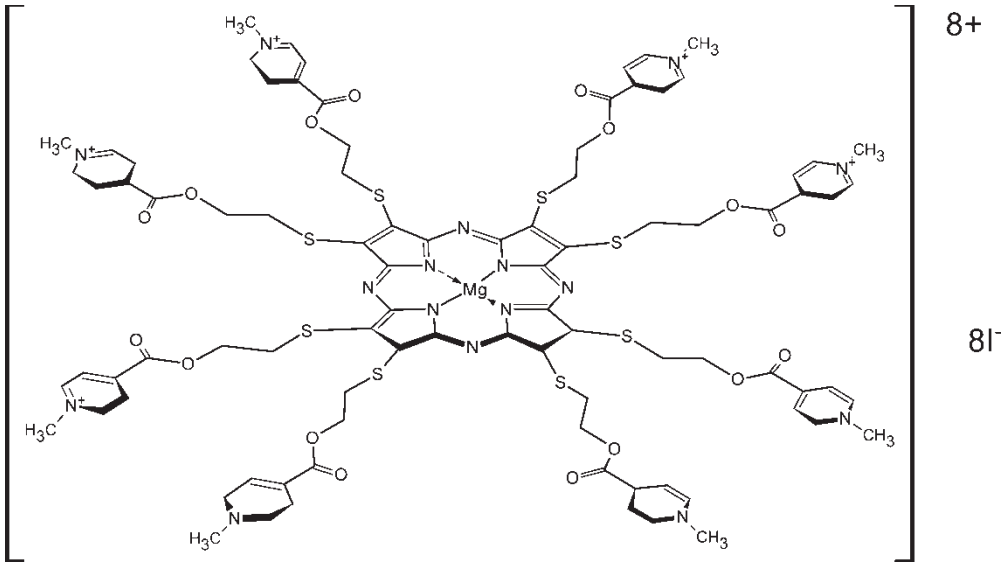

FIGURE 3 Octacationic porphyrazine (QMgPyPz).

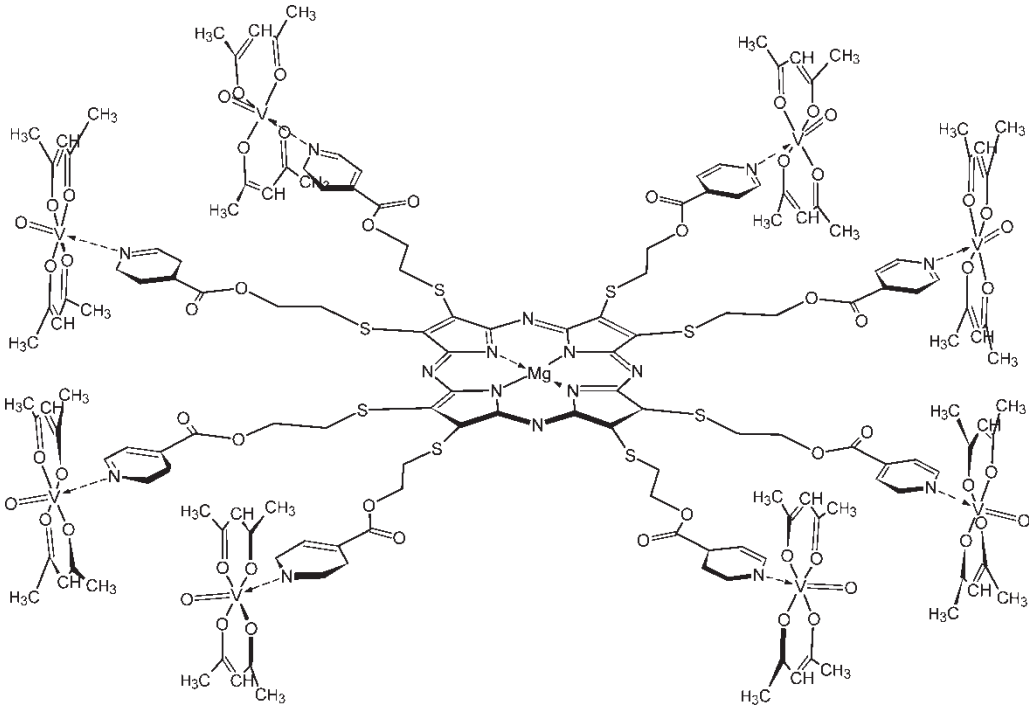

FIGURE 4 Nonanuclear supramolecular porphyrazine.

Downloaded At: 15:13 29 January 2011

$[VO(acac)_2]_8MgPyPz$ was obtained in high yield (76%) (Fig. 4).

The proposed structures of the octakis(pyridyl) derivative MgPyPz and the supramolecule are consistent with their spectral characterization; the visible absorption spectra of MgPyPz and the supramolecule in chloroform are similar. As $VO(acac)_2$ complexes are not expected to have intense absorptions comparable with the B- and Q-bands of porphyrazines, this result is meaningful. Although the Q-bands are known to be extremely sensitive to aggregation of the tetrapyrrole cores, complexation of pyridine units on the periphery has a negligible effect in this sense.

EPR Studies

The room temperature EPR experiments were designed to consist of three steps. In the first step, EPR spectra were recorded for the V^{4+} ($^2D_{3/2}$) ion-coordinated acetyl acetonate in solid powder form and in chloroform solution before coordination with the MgPyPz compound. In the second step, the MgPyPz compound was investigated to determine any inherent magnetic properties. Finally, the EPR signals were recorded from powder and chloroform solution forms of the $VO(acac)_2$-coordinated MgPyPz supramolecule, $[VO(acac)_2]_8MgPyPz$.

The first-derivative X-band EPR signals from the V^{4+}-coordinated acetyl acetonate, the MgPyPz compound itself and the supramolecule powder molecules with simulated spectra are shown in Fig. 5.

The intense resonance peak recorded from $VO(acac)_2$ powder has little asymmetry; that is the negative side of the spectrum is wider and shorter with respect to the positive side. The signal has no hyperfine peaks. Thus, it is not easy to identify the origin of this peak as the V^{4+} ion, but theoretical analysis leaves no room for doubt and proves the

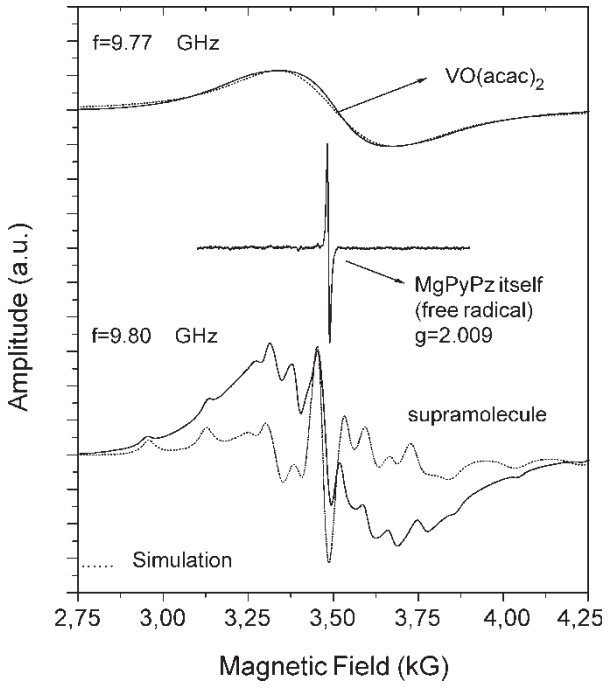

FIGURE 5 X-band EPR spectra of three powder forms at room temperature.

Downloaded At: 15:13 29 January 2011

presence of dipolar interaction with anisotropic Zeeman interaction.

The Hamiltonian describing the anisotropic Zeeman and dipolar interactions should include a third term theoretically (that is isotropic hyperfine interaction) and can be written as

$$H_{\text{aniso}} = \beta_e[(g_\perp(B_xS_x + B_yS_y) + g_\parallel(B_zS_z)] + \delta A(3\cos^2\theta - 1)S_zI_z + A_0(SI) \quad (1)$$

where $g_\perp$ and $g_\parallel$ are the Lande splitting factors corresponding to $B_\perp$ and $B_\parallel$, β_e is the Bohr magneton, S the total electronic angular momentum, I the total nuclear angular momentum, A_0 the isotropic hyperfine coupling constant and δA the dipolar constant expanded by an expression as given in the literature [38]. As the isotropic hyperfine interaction has no effective role here, it is neglected at theoretical fit studies.

The X-band EPR spectra of MgPyPz in powder and chloroform solution forms were recorded at room temperature before coordination with $VO(acac)_2$. Identical very narrow and weak peaks with small amplitude were recorded from both forms. The single peak recorded from the powder form can be seen in Fig. 5. The line width of the signal is just 6 G, and as for the amplitude the receiver gain of spectrometer is very high. The Lande splitting factor, $g = 2.009$, is very near that of free electrons ($g_e = 2.0023$), that is the observed resonance line is probably a free radical peak that may be formed as an impurity signal due to photolysis during synthesis.

The last group consists of experimental and theoretically well-fitted EPR signals of the $VO(acac)_2$-coordinated Mg-porphyrazine compound in powder form. The experimental spectrum has a characteristic and anisotropic curve that specifies uniaxial symmetry for a compound with $g_\perp$ slightly greater than $g_\parallel$. Both parallel and perpendicular parts of the spectrum contain hyperfine peaks. At the perpendicular part of the spectrum, seven hyperfine peaks are well resolved due to their location at the central region. For the parallel part, six hyperfine peaks are observed clearly at both sides of the perpendicular region. Eight hyperfine peaks are expected due to the interaction between the electronic spin of the magnetic electron and the nuclear spin of the $V^{4+}(I = 7/2)$ ion for both parallel and perpendicular parts of this porphyrazine compound. The other peaks are not well separated due to overlapping and line-broadening effects. The observed octet of lines from V^{4+} was not equally spaced due to second-order effects.

The Hamiltonian describing the anisotropic Zeeman and hyperfine interactions with anisotropic second-order corrections [38], respectively, can be written as

$$H_{\text{aniso}} = \beta_e[(g_\perp(B_xJ_x + B_yJ_y) + g_\parallel(B_zJ_z)] + A_\perp(I_xJ_x + I_yJ_y) + A_\parallel(I_zJ_z) + A_{\text{eff}}^2/(2g_{\text{eff}}\beta_e hf)\left[I(I+1) + M_I^2\right] \quad (2)$$

where h is the Planck constant, f the microwave frequency, M_I the nuclear momentum quantum number, and $A_\perp$ and $A_\parallel$ the hyperfine coupling constants for perpendicular and parallel parts, respectively.

In a powder system, each spin has almost the same properties as it would have in a single large crystal. However, the principal axes of crystallite components of the overall paramagnetic system may assume all possible orientations relative to the direction of the applied magnetic field. That is, the EPR spectrum can be expected to be spread over the entire field range ΔB (between $B_\perp$ and $B_\parallel$) determined by the principal g components of the system. Thus, for a single crystalline ensemble containing a paramagnetic center, the resonance field (B_{Res}) value can be calculated by introducing the angular-dependent parameters in the Hamiltonian (Eq. (2)). After simple mathematical manipulations:

$$\begin{aligned} B_{\text{Res}} &= g_e/g_{\text{eff}}\left\{hf/\beta_e - A_{\text{eff}}M_I/\beta_e + A_{\text{eff}}^2/2g_{\text{eff}}\beta_e\left[I(I+1)+M_I^2\right]\right\} \\ &= g_e/\left[\left(g_\parallel^2 - g_\perp^2\right)\cos^2\theta + g_\perp^2\right]^{1/2} \\ &\quad \times\left\{hf/\beta_e - \left[\left(A_\parallel^2 - A_\perp^2\right)\cos^2\theta + A_\perp^2\right]^{1/2}M_I/\beta_e \right. \\ &\quad \left. + \left[\left(A_\parallel^2 - A_\perp^2\right)\cos^2\theta + A_\perp^2\right]/2\beta_e\left[I(I+1)+M_I^2\right]\right\} \end{aligned} \quad (3)$$

where θ is the angle between the magnetic field and the symmetry axis direction of any particular spin species in the powder compound.

However, the number of paramagnetic centers making an angle θ with the field is proportional to $\sin\theta$. By using an additional weighting factor [39] and $\sin\theta$ together in Eq. (2), the following expression is obtained for the amplitude factor

$$\text{Amplitude factor} = \sin\theta \times \text{weighting factor} = \sin\theta\left(B_{\text{Res}}^2 - B_\parallel^2\right)/B_\parallel^2 \quad (4)$$

which is proportional to the number of paramagnetic centers giving a resonance absorption at B_{Res}.

As the resonance curves of each individual magnetic center have their own intrinsic line shape and width for powder systems, the line width and line shape characteristics of spectra are analyzed in detail by EPR spectroscopy. These curves reach to their maximum at the resonance field B_{Res}. That is,

regardless of how far it is from the exact resonance field, B_{Res}, any center can give absorption at any field even if it becomes undetectable experimentally. The contribution from any center to the whole absorption line at any field depends on the intrinsic line width. Therefore, we used an equation that is both M_I and angle dependent to obtain a theoretical fit for the line width characteristic of the lines [38, 40]

$$L = W_{\text{eff}}(\theta) + B_{\text{eff}}(\theta)M_I + CM_I^2 \tag{5}$$

where L is the line width and W_{eff}, B_{eff} and C are the coefficients. W_{eff} and B_{eff} are expanded due to their angular dependence as

$$\begin{aligned} W_{\text{eff}} &= \left[\left(W_{\parallel}^2 - W_{\perp}^2\right)\cos^2\theta + W_{\perp}^2\right]^{1/2}, \\ B_{\text{eff}} &= a(b - \cos^2\theta) \end{aligned} \tag{6}$$

where a is in terms of Gauss and takes any real value (plus or minus), and b is a unitless value between 0 and 1.

An angular-dependent $C_{\text{eff}}(\theta)$ value can be used to fit the experimental data, but for the simulations we did not need it because of the less effective role of the C parameter when it is compared with the other coefficients.

X-band EPR signals taken from $VO(acac)_2$ before coordination and from $[VO(acac)_2]_8MgPyPz$ supramolecules in chloroform solution with simulated spectra are shown in Fig. 6. The signals show eight well-resolved hyperfine peaks as expected due to interaction between the electronic spin of the magnetic electron and the nuclear spin of the $V^{4+}(I = 7/2)$ ion. Hyperfine lines do not show symmetrical character that is line width and amplitude of every peak changes from the low-field to the high-field region. Varying shifts from a constant hyperfine splitting (A_0) value between each transition line are also observed.

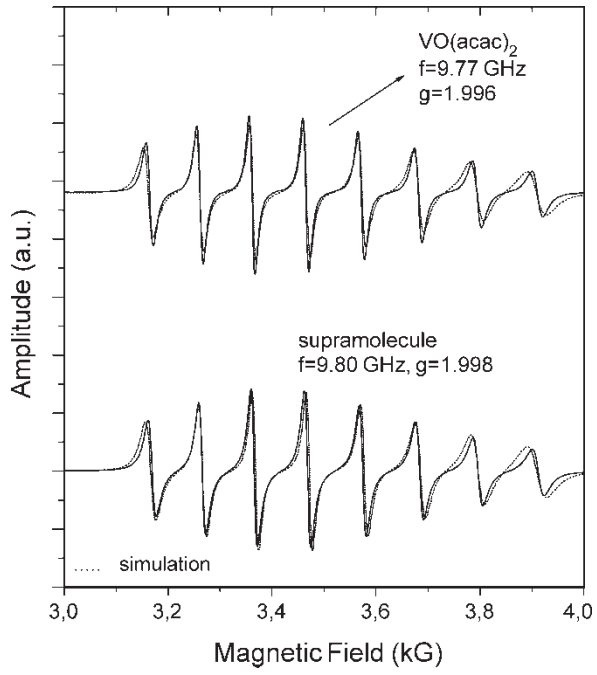

FIGURE 6 X-band EPR spectra of $VO(acac)_2$ and the supramolecular complex compound in chloroform solution at room temperature.

The experimental $VO(acac)_2$ spectrum and the theoretical fit studies prove that very significant line-narrowing effects are valuable for the hyperfine peaks. The reason for the line-narrowing effects must be the decreasing amount of dipolar interaction between the magnetic moments of the atom and the electron. As the chloroform solution increases the average separation between the magnetic ions, the dipolar effects get weaker and under these conditions line-narrowing effects can be expected.

In Fig. 5, the two experimental spectra recorded from $VO(acac)_2$ and the supramolecule show very similar characteristic line shapes. A similar approach is useful for their spin Hamiltonian and line width parameters. In particular, when we compare the spectra of the supramolecule in powder (Fig. 5) and in solution forms, a significant change is seen on going from anisotropic to isotropic behavior. In chloroform solution, this behavior is due to the faster random (rotational) motion of $VO(acac)_2$-coordinated MgPyPz molecules compared to the microwave frequency. Consequently, a microwave photon sees magnetic energy splitting averaged out over the solid angle of the spins with respect to the external field; that is, magnetic parameters like g and A show themselves as if they are isotropic. Thus, in solution, the spectrum has isotropic parameters as shown in Fig. 6, in contrast to the anisotropic parameters for the solid powder form.

The Hamiltonian describing the isotropic Zeeman and isotropic hyperfine interaction with second-order corrections [38], respectively, can be written as

$$\begin{aligned} H_{\text{iso}} &= g\beta_e BS + A_0 SI + A_0^2/(2g\beta_e hf) \\ &\quad \times \left[I(I+1) + M_I^2\right] \\ M_I &= -I, -I+1, \ldots, -1+I, +I \end{aligned} \tag{7}$$

The main purpose of this EPR study of a nonanuclear supramolecular compound is to prove the coordination of $VO(acac)_2$ through peripheral pyridine donors. When we compare the spectra taken from $VO(acac)_2$ itself and supramolecular porphyrazine, the axially symmetric character is not seen in the spectra recorded for $VO(acac)_2$ powder form in Fig. 5. From the literature, it is well known that $VO(acac)_2$ has square pyramidal geometry and V^{4+} is not in an octahedral site [41]. In the supramolecular complex, $VO(acac)_2$ molecules attain an octahedral geometry and uniaxial symmetry is exactly provided when the molecules are

Downloaded At: 15:13 29 January 2011

TABLE I EPR parameters for $VO(acac)_2$ and the supramolecular complex

	$g_\perp$	$g_\parallel$	G	$a_\perp$ (G)	$a_\parallel$ (G)	a_0 (G)
$VO(acac)_2$ in powder form	1.993	1.980	1.9867	–	–	$\delta A = 60$
$VO(acac)_2$ in solution form	–	–	1.9960	–	–	105.5
$VO(acac)_2$-coordinated supramolecule in powder form	1.998	1.963	1.9863	65	176	102
$VO(acac)_2$-coordinated supramolecule in solution form	–	–	1.9980	–	–	105

coordinated to MgPyPz. Here, it is possible that there may be some uncoordinated $VO(acac)_2$ groups. The theoretical fit studies carried out by using the Hamiltonian Eq. (2) shows that this consideration is not valid due to the disappearance of dipolar interactions, which must be the result of significant separation of the coordinated $VO(acac)_2$ groups from the peripheral pyridine units. If a significant number of $VO(acac)_2$ groups were not coordinated, we would record a similar intensive single peak without hyperfine lines as observed for the uncoordinated $VO(acac)_2$ molecule.

The theoretically best-fit EPR and line width parameters are given in Tables I and II, respectively. Table I shows that the spin Hamiltonian parameters A and g are in agreement with the values generally observed for vanadyl complexes with square pyramidal geometry [40]. There is a trend that $g_\parallel < g_\perp < g_e$, indicating the presence of an unpaired electron in the d_{xy} orbital [42]. It is understood from Table I that for an unpaired electron this trend still continues due to the octahedral geometry in the $VO(acac)_2$-coordinated supramolecule.

In Table I, the isotropic g and A_0 parameters are estimated as average values for powder molecules given in rows 1 and 3. We have calculated their values from Eqs. (8) and (9).

$$g = (g_\parallel + 2g_\perp)/3 \tag{8}$$

$$a_0 = (a_\parallel + 2a_\perp)/3 \tag{9}$$

The best fits of all theoretical EPR spectra with experimental signals have been obtained by using the Lorentzian line shape function according to the results taken by using the Gaussian line shape function and all computer simulation programs have been written by Matlab.

In summary, we can say that both spectral and EPR analysis results confirm the presence of identical pyridine-coordinated $VO(acac)_2$ paramagnetic centers attached to the peripheral positions of the MgPyPz core.

Conclusion

A convenient synthetic route to the substitution of the porphyrazine core with eight pyridyl moieties bridged through flexible ethylthio ester units has been accomplished. It has also been shown that these pyridyl groups can be either quaternized to yield octacationic porphyrazines or capped with $VO(acac)_2$ complexes to prepare a nonanuclear supramolecular product. Work on the interaction of the octacationic products with DNA molecules is under way.

EXPERIMENTAL

All reagents and solvents were of reagent grade and used as received. EPR spectra were recorded by a conventional X-band ($\nu = 9.5$–9.85 GHz) Bruker EMX spectrometer using an ac magnetic modulation technique. FTIR measurements were performed with a KBr disk with a Mattson Genesis II FTIR spectrophotometer, UV–visible measurements were carried out with Unicam double-beam spectrophotometer, elemental analysis by a Carlo Erba 1106 instrument, and ^{1}H NMR measurements were carried out in DMSO-d_6 or $CDCl_3$ using a Bruker AC-250 MHz instrument. Octakis(hydroxyethylthio)porphyrazinato magnesium, MgOHPz, was synthesized according to the procedure given in the literature [33, 34].

Octakis(4-pyridoxyethylthio)porphyrazinato Magnesium, MgPyPz

A mixture of MgOHPz 0.5 mmol (472 mg), DCCI 12 mmol (2.472 g), *p*-TSA 0.5 mmol (0.095 g) and pyridine 4-carboxylic acid (isonicotinic acid) 12 mmol (1.476 g) was stirred in 40 ml dry pyridine for about 7 days at ambient temperature under a nitrogen atmosphere. Dicyclohexylurea byproduct and unreacted pyridine 4-carboxylic acid were

TABLE II Line width parameters for $VO(acac)_2$ and the supramolecular complex

	B_{eff} (G)	W (G)	$W_{(G)}$	$W_\top$ (G)	C (G)
$VO(acac)_2$ in powder form	0	–	20	225	0
$VO(acac)_2$ in solution form	$-1.7(0.9 - \cos^2\theta)$	14	–	–	1
$VO(acac)_2$-coordinated supramolecule in powder form	$-5\cos^2\theta)$	–	35	33	0.5
$VO(acac)_2$-coordinated supramolecule in solution form	$-1.5(1 - \cos^2\theta)$	14.5	–	–	1.1

Downloaded At: 15:13 29 January 2011

precipitated and filtered off and the dark green filtrate was evaporated to dryness under reduced pressure. The crude product was stirred in a mixture of 1:1 ethanol–cyclohexane (v/v) for 2 days at 0 °C to remove the remaining dicyclohexylurea. Further purification was achieved by column chromatography on silica gel with $CHCl_3$/methanol (3/1) as eluent. Yield: 285 mg, 35%. ^{1}H NMR (250 MHz, $CDCl_3$): δ/ppm: 4.39 (t, 2H, SCH_2 $J = 4.39$ Hz), 4.81 (t, 2H, OCH_2 $J = 5.09$ Hz), 7.43 (d, 2H, py $J = 5.18$ Hz) and 8.17 (d, 2H, py $J = 5.55$ Hz). UV/vis ($CHCl_3$), λ_{max}/nm($\varepsilon \times 10^4$/M^{-1} cm^{-1}) : 372(10.7), 672 (9.7). FAB-MS 1788 $(M + 2)^+$. Anal. Calc. for $C_{80}H_{64}O_{16}S_8Mg$(%): C, 53.79; H, 3.61; N, 12.55. Found: C, 53.62; H, 4.07; N, 12.21. ν(KBr) cm^{-1}: 3050 (CH, py), 2945–2960 (CH), 1727 (C═O), 1284 (C—O).

Metal-free Porphyrazine, H_2PyPz

MgPyPz (0.1 mmol, 178 mg) was dissolved in 5 ml of 6 M H_2SO_4 at 0 °C and stirred at this temperature for 1 h. Then the reaction mixture was added dropwise into 20 g crushed ice. The resultant mixture was neutralized first with ammonia solution (25%) and then with 1 M NaOH. The precipitated product was filtered off, washed with water and then dissolved in chloroform. The chloroform solution was dried over anhydrous sodium sulfate, filtered and evaporated to dryness to give purple colored metal-free porphyrazine. The crude product was purified by column chromatography (silica gel, chloroform/-methanol 1:10). Yield: 120 mg, 85%. ^{1}H NMR (250 MHz, $CDCl_3$): δ/ppm: −1.9 (broad s, N—H), 4.41 (t, 2H, SCH_2 $J = 4.48$ Hz), 4.87 (t, 2H, OCH_2 $J = 5.14$ Hz), 7.41 (d, 2H, py $J = 5.25$ Hz) and 8.23 (d, 2H, py $J = 5.63$ Hz). UV/vis ($CHCl_3$), λ_{max}/nm($\varepsilon \times 10^4$/M^{-1} cm^{-1}) : 372(7.2), 640(5.2), 704(6.3). Anal. Calc. for $C_{80}H_{66}N_{16}O_{16}S_8$(%): C, 54.45; H, 3.70; N, 12.56. Found: C, 54.62; H, 3.87; N, 12.41. ν(KBr) cm^{-1}: 3293 (N—H), 3050 (CH, py), 2945–2960 (CH), 1727 (C═O), 1284 (C—O).

Octacationic Porphyrazine, QMgPyPz

A mixture of 0.1 mmol (178 mg) of MgPyPz and 25.6 mmol (1.6 mL) of iodomethane was stirred in (20 mL) dichloromethane at room temperature for 24 h under nitrogen in the dark [36]. The precipitate formed was separated from the almost colorless solution by decantation. The solid product was washed several times first with cold dichloromethane and then with diethyl ether. Yield: 140 mg, 68%. ^{1}H NMR (250 MHz, DMSO-d_6): δ/ppm: 4.29 (s, CH_3), 4.44 (t, 2H, SCH_2 $J = 4.53$ Hz), 4.91 (t, 2H, OCH_2 $J = 5.23$ Hz), 7.41 (d, 2H, py $J = 5.27$ Hz) and 8.23 (d, 2H, py $J = 5.65$ Hz). UV/vis(H_2O), λ_{max}/nm($\varepsilon \times 10^4$/M^{-1} cm^{-1}) : 374(7.8), 674(4.7). Anal. Calc. for $C_{88}H_{88}N_{16}O_{16}S_8Mg$(%): C, 55.40; H, 4.62; N, 11.75. Found: C, 55.62; H, 4.87; N, 11.88%. ν(KBr) cm^{-1}: 3050 (CH, py), 2945–2960 (CH), 1727 (C═O), 1284 (C—O).

Nonanuclear Supramolecular Porphyrazine, [VO(acac)$_2$ 4-PyCOOCH$_2$CH$_2$S]$_8$MgPz

A mixture (1:10 ratio) of 0.1 mmol of MgPyPz (178 mg) and 1 mmol (265 mg) of VO(acac)$_2$ was refluxed in (40 mL) chloroform for 6 h. The reaction was monitored by TLC (silica; 1/50 MeOH/$CHCl_3$). When the solvent was removed, a green, crude product was obtained. During the purification process by column chromatography on silica gel, any unreacted VO(acac)$_2$ was first eliminated by using MeOH/$CHCl_3$ (1:50) as eluent. Then the main product was eluted with MeOH/$CHCl_3$ (1:5). Yield: 250 mg, 75%. Anal. Calc. for $C_{160}H_{176}N_{16}O_{56}S_8V_8Mg$(%): C, 49.19; H, 4.54; N, 5.74. Found: C, 49.23; H, 4.06; N, 5.97%. UV/vis (CH_2Cl_2), λ_{max}/nm($\varepsilon \times 10^4$/M^{-1} cm^{-1}) : 372(5.3), 672(4.4). ν(KBr) cm^{-1}: 3050 (CH, py), 2945–2960 (CH), 1727 (C═O), 1284 (C—O), 1527 and 1373 (acac), 995 (V═O).

EPR Measurements

The powder and chloroform solution forms of VO(acac)$_2$, MgPyPz and the nonanuclear supramolecular compound were investigated by EPR at room temperature.

References

[1] Purello, R.; Gurrieri, S.; Lauceri, R. *Coord. Chem. Rev.* **1999**, *190–192*, 683.
[2] Tjahjono, D. H.; Mima, S.; Akutsu, T.; Yoshioka, N.; Inoue, H. *J. Inorg. Biochem.* **2001**, *85*, 219.
[3] Malinovski, V.; Tumir, L.; Piantanida, I.; Zinic, M.; Schneider, H. *Eur. J. Org. Chem.* **2002**, 3785.
[4] Vzorov, A.; Marzilli, L. G.; Compans, R. W.; Dixon, D. W. *Antiviral Res.* **2003**, *59*, 99.
[5] Arthanari, H.; Bolton, P. H. *Anti-Cancer Drug Design* **1999**, *14*, 317.
[6] Zemcik, P.; Miletin, M.; Ponec, J.; Kostka, M.; Fiedler, Z. *J. Photochem. Photobiol. A: Chem.* **2002**, *155*, 127.
[7] Gandini, C. M. S.; Yushmanov, V. E.; Perussi, J. R.; Tabak, M.; Borissevitch, I. E. *J. Inorg. Biochem.* **1999**, *73*, 35.
[8] Izbicka, E.; Nishioka, D.; Marcell, V.; Raymond, E.; Davidson, K. K.; Lawrence, R. A.; Wheelhouse, R. T.; Hurley, L. H.; Wu, R. S.; Von Hoff, D. D. *Anti-Cancer Drug Design* **1999**, *14*, 355.
[9] Anderson, E. M.; Barett, A. G. M.; Hoffman, B. M. *J. Inorg. Biochem.* **2000**, *80*, 257.
[10] Tabata, M.; Nyarko, E. *J. Porphyrins Phthalocyanines* **2001**, *5*, 873.
[11] Song, R.; Sang-Kim, Y.; Soo Sohn, Y. *J. Inorg. Biochem.* **2002**, *83*, 83.
[12] Bellec, N.; Montalban, A. G.; Williams, D. B.; Cook, A. S.; Anderson, M. E.; Feng, X.; Barrett, A. G. M.; Hoffman, B. M. *J. Org. Chem.* **2000**, *65*, 1774.
[13] Anderson, M. E.; Barett, A. G. M.; Hoffman, B. M. *Inorg. Chem.* **1999**, *38*, 6143.

Downloaded At: 15:13 29 January 2011

[14] Castriciano, M.; Romeo, A.; Romeo, R.; Scolaro, L. M. *Eur. J. Inorg. Chem.* **2002**, 531.
[15] Scolaro, L. M.; Donato, C.; Castriciano, M.; Romeo, A.; Romeo, R. *Inorg. Chim. Acta* **2000**, *300–302*, 978.
[16] Lensen, M. C.; Castriciano, M.; Coumans, R. G.; Foekema, J.; Rowan, A. E.; Scolaro, L. M.; Nolte, R. J. M. *Tetrahedron Lett.* **2002**, *43*, 9351.
[17] Toma, H. E.; Araki, K. *Coord. Chem. Rev.* **2000**, *96*, 307.
[18] Prodi, A.; Indelli, T. M.; Kleverlaan, C. J.; Alessio, E.; Scandola, F. *Coord. Chem. Rev.* **2002**, *229*, 51.
[19] Iengo, E.; Zagrando, E.; Alessio, E. *Eur. J. Inorg. Chem.* **2003**, 2371.
[20] Seotsanyana, I. M.; Kuznetsova, N.; Nyokong, T. *J. Photochem. Photobiol. A: Chem.* **2001**, *140*, 215.
[21] Toyama, M. M.; Franco, M.; Catalani, L. H.; Araki, K.; Toma, E. H. *J. Photochem. Photobiol. A: Chem.* **1998**, *118*, 11.
[22] Araki, K.; Araujo, L. A.; Toyama, M. M.; Franco, M.; Azavedo, C. M. N.; Angnes, L.; Toma, E. H. *J. Porphyrins Phthalocyanine* **1998**, *2*, 467.
[23] Prodi, A.; Kleverlaan, C. J.; Indelli, T. M.; Scandola, F. *Inorg. Chem.* **2001**, *40*, 3498.
[24] Alessio, E.; Macchi, M.; Heath, S. L.; Marzilli, L. G. *Inorg. Chem.* **1997**, *36*, 5614.
[25] Iengo, E.; Minatel, R.; Milani, B.; Marzilli, L. G.; Alessio, E. *Eur. J. Inorg. Chem.* **2001**, 609.
[26] Winnischofer, H.; Engelman, F. M.; Toma, E. H.; Araki, K.; Rechenberg, R. H. *Inorg. Chim. Acta* **2002**, *338*, 27.
[27] Sakallariou, E. G.; Montalban, A. G.; Meunier, H. G.; Ostler, B. R.; Rumbles, G.; Barret, A. G. M.; Hoffman, B. M. *J. Photochem. Photobiol. A: Chem.* **2000**, *136*, 185.
[28] Selby, H. H.; Roland, B. K.; Zheng, Z. *Acc. Chem. Res.* **2003**, *36*, 933.
[29] Berber, G.; Cammidge, A. N.; Chambrier, I.; Cook, M. J.; Hough, P. W. *Tetrahedron Lett.* **2003**, *44*, 5527.
[30] Kimura, M.; Hamakawa, T.; Hanabusa, K.; Shirai, H.; Kobyashi, N. *Inorg. Chem.* **2001**, *40*, 4775.
[31] Burchfield, J. M.; Du, J. L.; More, K. M.; Eaton, S. S.; Eaton, G. R. *Inorg. Chim. Acta* **1997**, *263*, 23.
[32] Eichhorn, H.; Rutloh, M.; Wöhrle, D.; Stumpe, J. *J. Chem. Soc., Perkin Trans. 2*, **1996**, 1801.
[33] Sağlam, Ö.; Gül, A. *Polyhedron* **2000**, *20*, 269.
[34] Akkuş, H.; Gül, A. *Transition Met. Chem.* **2000**, *26*, 689.
[35] Öztürk, R.; Gül, A. *Tetrahedron Lett.* **2004**, *45*, 947.
[36] Polat, M.; Gül, A. *Dyes Pigments* **1999**, *45*, 195.
[37] Ebdon, J. R.; Guisti, L.; Hunt, B. J.; Jones, M. S. *Polym. Degradation Stability* **1998**, *60*, 401.
[38] Weil, J. A.; Bolton, J. R.; Wertz, J. E. *Electron Paramagnetic Resonance*; John Wiley and Sons Inc.: New York, 1994.
[39] Abragam, A.; Bleaney, B. *EPR of Transition Ions*; Oxford University Press: Oxford, 1970.
[40] Heucher, R.; Chandramouli, G. V. R.; Manoharan, P. T. *J. Porphyrins Phthalocyanine* **1998**, *2*, 423.
[41] Carrano, C. J.; Nunn, C. M.; Quan, R.; Bonadies, J. A.; Pecoraro, V. L. *Inorg. Chem.* **1990**, *29*, 941.
[42] Gangadharmath, U. B.; Annigeri, S. M.; Naik, A. D.; Revankar, V. K.; Mahale, V. B. *J. Mol. Struct. (Theochem.)* **2001**, *572*, 61.

Downloaded At: 15:13 29 January 2011